International Scholarly Research Network
ISRN Nanotechnology
Volume 2011, Article ID 582534, 7 pages
doi:10.5402/2011/582534

Research Article

Preparation of TiO_2 Nanoparticle/Nanotube Composites via a Vapor Hydrolysis Method and Their Photocatalytic Activities

Weiwei Yu,[1] Sujun Yuan,[1] Yaogang Li,[2] Qinghong Zhang,[2] and Hongzhi Wang[1]

[1] *State Key Laboratory for Modification of Chemical Fibers and Polymer Materials, Donghua University, Shanghai 201620, China*
[2] *Engineering Research Center of Advanced Glasses Manufacturing Technology, MOE, Donghua University, Shanghai 201620, China*

Correspondence should be addressed to Qinghong Zhang, zhangqh@dhu.edu.cn and Hongzhi Wang, wanghz@dhu.edu.cn

Received 23 June 2011; Accepted 15 August 2011

Academic Editors: A. Hu, A. N. Obraztsov, A. Swami, and N. Tabet

TiO_2 nanoparticle/nanotube composites were prepared by a vapor hydrolysis method and were characterized by X-ray diffraction, transmission electron microscopy, and N_2 isothermal adsorption-desorption. The well-crystallized TiO_2 nanoparticles were uniformly deposited onto the surface of TiO_2 nanotubes. The photocatalytic activity of the composites was evaluated by the degradation of acid red G and phenol solution under UV irradiation. The results showed that the photocatalytic activities of the modified composites were significantly enhanced compared to the pristine nanotubes. In particular, the 50 wt% TiO_2 nanoparticle/nanotube composite obtained at 120°C exhibited a remarkable ARG degradation efficiency of 90% after irradiation for 30 minutes and a phenol degradation efficiency of 93% after irradiation for 2 hours.

1. Introduction

With the development of technology, the environmental pollution deriving from artificial products has become a serious problem. In response to this, materials which can absorb the harmful pollutants irreversibly and eliminate them completely have been developed. Among the various kinds of catalysts, the incorporation of photocatalysts with adsorbents has gained more attention [1], which offers a new design of a photocatalytic system. Although some nanocomposites with high adsorbing capacities as well as high photocatalytic activities have been prepared, such as TiO_2/zeolite [2], TiO_2/activated carbon [3], and TiO_2/SiO_2 [4], the exploring of new composites for the application in more industrial purposes is expected. As established, TiO_2 nanotubes (TNTs) have been widely used as adsorbents in different fields because of their tailored pore structures and high specific surface areas [5, 6]. However, pristine TNTs are almost without photocatalytic activities and their applications in photocatalysis are limited. There are two main techniques to improve the photocatalytic properties of TNTs: improving crystallinity of the nanotubes and substance-loaded interaction [7–9].

Calcination and hydrothermal treatment have been always used to enhance the crystallinity of the nanotubes [10–12]. Nevertheless, using these two methods is easy to destroy the nanotubular structure and results in significantly reduced specific surface area of the nanotubes [10–13]. In order to solve this problem, Wang et al. [13] have reported a chemical morphology freezing method to protect TNTs from unavoidable collapse by filling them with carbon and coating them with a silica sheath. They have demonstrated that perfectly crystallized and open-ended TiO_2 nanotubes have been maintained during the calcination process. But the TNTs obtained in this method are covered with a layer of SiO_2 and the photocatalytic reaction is restricted to the inside of nanotubes, which limit the further application of the nanotubes. On the other hand, the photocatalytic modification of TNTs has also been reported, including ZnO-supported [14], Au (Pt)-doped [15, 16], and PbS surface coated nanotubes [7]. These composites still have some shortcomings in applications, such as the photocorrosion of ZnO or the high cost of the precious metals. In contrast, TiO_2 may be more appropriate as a photocatalyst for the modification because of its high photosensitivity, nontoxicity, and low cost [17–21]. Therefore, we assume that

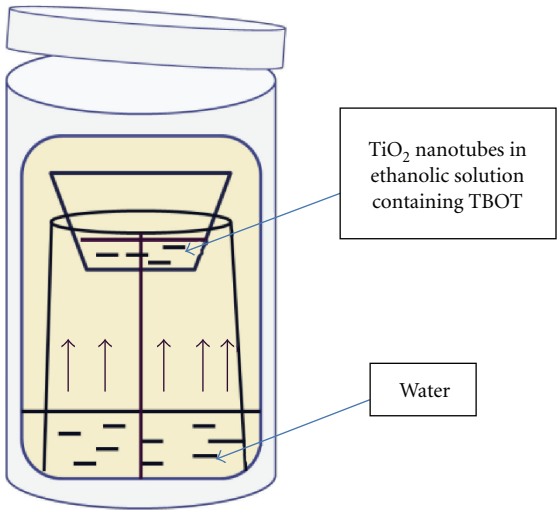

Scheme 1: Illustration of vapor hydrolysis setup.

a nanoparticle/nanotube composite consisting of only TiO_2 will be a good catalyst in the environmental remediation. To the best of our knowledge, there are few reports on the preparation of TiO_2 nanoparticle/nanotube composites.

A direct synthesis of TiO_2 nanoparticle/nanotube composites through a vapor hydrolysis method was studied in this work. The degradations of acid red G (ARG) and phenol under UV illumination were used as model reactions to evaluate the photocatalytic activities of the composites, and the effects of the vapor hydrolysis temperature and TiO_2 loading content were investigated in detail.

2. Experimental

2.1. Preparation. All of the chemicals used were analytical-grade reagents without any further purification. TNTs were synthesized by the hydrothermal method [22], and the typical synthetic procedure is described as follows: a total of 0.1 g P-25 powder (Degussa, composed of TiO_2 with 80% in anatase and 20% in rutile phase) was placed into 60 mL of 10 M NaOH aqueous solution. After vigorous stirring, the mixture was transferred into a hydrothermal Teflon-lined autoclave and heated to 110°C for 24 hours. The product was collected by centrifugation and washed by deionized water for several times until the pH reached 7-8. The remaining sodium titanate phase was further washed by 0.1 M HNO_3, deionized water and ethanol to exchange the remaining Na^+ thoroughly. Finally, the washed TNTs were dried at 80°C under vacuum for 24 hours.

TiO_2 nanoparticle/nanotube composites were prepared through a vapor hydrolysis method illustrated in Scheme 1. 0.1 g of as-prepared TNTs was dispersed into 7 mL ethanolic solution which contained 100 μL to 200 μL tetrabutyl titanate (TBOT). After an ultrasonic dispersion for 3 minutes, the solution was quickly transferred into the vapor-phase hydrolysis device. 3 mL of deionized water was added at the bottom of the device to act as the vapor producing liquid phase when the temperature was elevated. The closed device was heated at different temperature (100°C, 120°C, and 150°C, resp.) for 12 h. The final products were collected by centrifugation and rinsed several times with deionized water and ethanol to remove impurities and then dried under vacuum at 80°C for 12 hours. For comparison, the TNTs without TiO_2 loadings and the bare TiO_2 nanoparticles were also obtained through the vapor hydrolysis method. All the samples were named according to the content of TiO_2 loading and the vapor hydrolysis temperature. For instance, the sample of pristine TNTs steamed at 100°C was denoted as TNTs-0-100 and the composite with 50 wt% of TiO_2 loading steamed at 100°C was denoted as TNTs-50-100. Here, the content of TiO_2 loading was based on the amount of the TiO_2 derived from the hydrolysis of TBOT in the preparation, excluding the crystallization of the nanotubes.

2.1.1. Characterization. The crystalline phase of the as-prepared products was identified by X-ray diffraction (Model D/Max-2550, Rigaku Co. Tokyo, Japan) using Cu K α radiation (λ = 1.5406 Å) at 40 kV and 100 mA. The morphologies of the TiO_2 nanoparticle/nanotube composites were observed by high-resolution transmission electron microscope (HRTEM) (Model JEM-2100F, JEOL, Tokyo, Japan), and the specific surface area was calculated by the Brunauer-Emmett-Teller (BET) method. The samples were outgassed for 24 hours at 150°C to remove loosely adsorbed species prior to N_2 isothermal adsorption-desorption. Pore size distribution and pore volume were calculated by the Barrett-Joyner-Halenda (BJH) method according to the measured isothermal adsorption-desorption (Model Autosorb-1MP, Quantachrome Instruments Co., USA).

2.2. Photocatalytic Experiment. The photocatalytic activity of TiO_2 nanoparticle/nanotube composites was evaluated by the degradation of two organic pollutants: ARG and phenol. Firstly, the experiment was carried out in a Pyrex photoreactor which contained 0.1 g of the photocatalysts and 500 mL of 50 ppm aqueous ARG (phenol). Prior to the irradiation, the solution was stirred in the dark for 20 minutes to reach the adsorption-desorption equilibrium [23, 24]. Then, a 300 W mediate pressure Hg lamp without a filter was used as a source of UV light and O_2 was bubbled into aqueous suspension at a flow rate of 100 mL min^{-1}. The suspensions were collected at regular intervals and separated through centrifugation. The concentration of the ARG solution was measured by a UV-vis spectrophotometer at the wavelength of 530 nm (Model Lambda 35, Perkin Elmer Co., USA). The concentration of phenol solution was monitored at wavelength of 270 nm.

3. Results and Discussions

3.1. The Formation Mechanism of TiO_2 Nanoparticle/Nanotube Composites. The main method of vapor hydrolysis was illustrated in Scheme 1, and the formation mechanism could be described as follows. The ethanolic solution of TBOT which served as the Ti precursor and the deionized water were put into the bottom of the vapor-phase hydrolysis

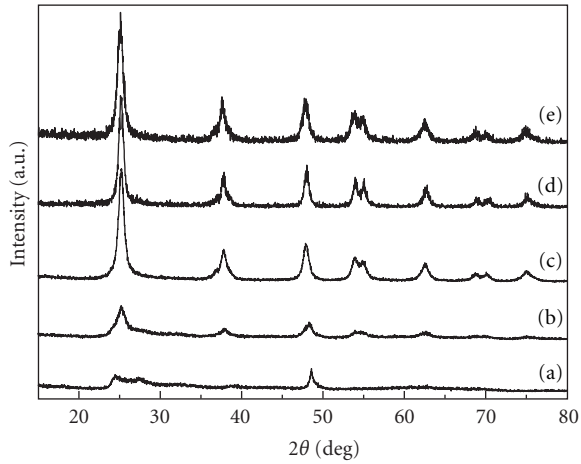

Figure 1: XRD patterns of TNTs (a), TNTs-0-100 (b), TNTs-0-120 (c), TNTs-0-150 (d), and TNTs-50-120 (e).

device together. As the temperature rose, the ethanol evaporated first due to its low boiling point and TBOT was adsorbed onto the surface of the TiO_2 nanotubes. When the boiling point of water was reached, TBOT would be hydrolyzed by the water vapor, and the well-crystallized anatase TiO_2 nanoparticles would be formed if the reaction temperature was raised further. Meanwhile, some supporting TiO_2 nanotubes would also crystallize into anatase TiO_2 and kept in a unique tube-like morphology.

3.2. Morphologies and Structural Analysis of TiO_2 Nanoparticle/Nanotube Composites. The X-ray diffraction patterns of the samples obtained under different conditions were shown in Figure 1. Compared to the weak peaks of pristine TNTs (Figure 1(a)), the characteristic XRD patterns for TiO_2 crystallites could be observed from Figure 1(b) to Figure 1(d). The peaks at 2θ of 25.4°, 37.9°, 48.1°, 54.1°, 55.2°, and 62.7° were corresponding to the (101), (004), (200), (105), (211), and (204) crystal planes of anatase TiO_2, respectively. It was demonstrated that the anatase TiO_2 was formed through the vapor hydrolysis process. When the reaction temperature was raised, the intensity of the characteristic peaks increased obviously, which indicated that the crystallization of the TNTs had improved. Moreover, a good crystallinity of TNTs-50-120 was noticed as well (showed in Figure 1(e)) and its intensity of the peaks had no visible change compared to that of TNTs-0-120. The actual TiO_2 loading of the TiO_2 nanoparticle/nanotube composites was derived from the hydrolysis of TBOT and the crystallization of the TiO_2 nanotubes. It was suggested that the TiO_2 nanoparticles obtained from the hydrolysis of TBOT was in anatase phase and the size of them was close to that of the TiO_2 crystalline in the TNTs.

The TEM image of the TNTs was observed in Figure 2(a). The pristine nanotubes presented a hollow tubular structure with two open ends. The length of the nanotubes ranged from 100 to 400 nm, and the average diameters ranged between 6 and 8 nm. Most of the TNTs were multiwalled and in the form of bundles [25–27]. After vapor hydrolysis at 100°C for 12 hours, the TNTs with TiO_2 nanoparticles could be found in Figure 2(b). The multilayered nanostructure of the TNTs was reopened in a mild way during the vapor hydrolysis process, and some of the tubes transformed into small flakes. The flakes would load onto the surface of the nanotubes, crystallize, and reunite. The corresponding high-resolution TEM image of TNTs-0-100 was showed in Figure 2(c). The clear lattice structure of the TiO_2 nanoparticles and nanotubes was formed which indicated that both the TNTs and the flakes derived from the TNTs had crystallized in the vapor hydrolysis process. The spacing between adjacent lattice fringes was 0.34 nm, which was close to the basal spacing of the plane (101) of anatase TiO_2 [28]. Moreover, Figure 2(d) showed the TEM micrographs of TNTs-23-120. The amount of TiO_2 nanoparticles in TNTs-23-120 had increased apparently. When TBOT hydrolyzed, the formed TiO_2 nanoparticles were gradually loaded onto the surface of TNTs at random. Meanwhile, the growth in size of the TiO_2 nanoparticles deposited onto the surface of the nanotubes could be seen when the vapor hydrolysis temperature increased.

Table 1: Summary of the specific surface area, pore volume, and pore diameter of the as-prepared samples.

Samples	S_{BET} ($m^2 \cdot g^{-1}$)[a]	V[b] ($cm^3 \cdot g^{-1}$)	D[c] (nm)
TNTs	463	2.18	14.9
TNTs-0-100	356	1.83	17.8
TNTs-0-120	185	0.65	12.0
TiO_2-23-100	348	1.73	16.3
TiO_2-30-100	331	1.62	16.2
TiO_2-50-100	305	1.42	16.1
TiO_2-23-120	183	0.52	9.8
TiO_2-30-120	177	0.48	9.6
TiO_2-50-120	121	0.46	8.0

[a]Specific surface area; [b]pore volume; [c]pore diameter.

The specific surface area, pore volume, and pore size distribution of the samples were characterized by nitrogen adsorption and desorption isotherms. As shown in Figure 3, the nitrogen adsorption-desorption isotherms of the samples had a small hysteresis loop at a relative pressure range of 0.8–0.9, which was a typical characteristic of mesoporous material. The corresponding BJH desorption pore size distributions were also plotted alongside each of the isotherms. The specific surface area of the pristine TNTs was 463 $m^2 \cdot g^{-1}$, and the pore sizes were mainly concentrated at about 14.9 nm, which suggested that the TNTs had a relatively high surface-to-volume ratio. As shown in Table 1, TNTs-0-100 still retained a high specific surface area of 356 $m^2 \cdot g^{-1}$. Moreover, with the increase of TiO_2 loading (from 23 to 50 wt%), the specific surface area of the samples declined gradually. It could be assumed that the TiO_2 nanoparticles formed after the hydrolysis of TBOT had gathered onto the pore structure of TiO_2 nanotubes. Nevertheless, when the vapor hydrolysis temperature was elevated to 120°C, the specific surface area of the TNTs dropped from 356 $m^2 \cdot g^{-1}$ to 185 $m^2 \cdot g^{-1}$ and the corresponding pore size reduced from

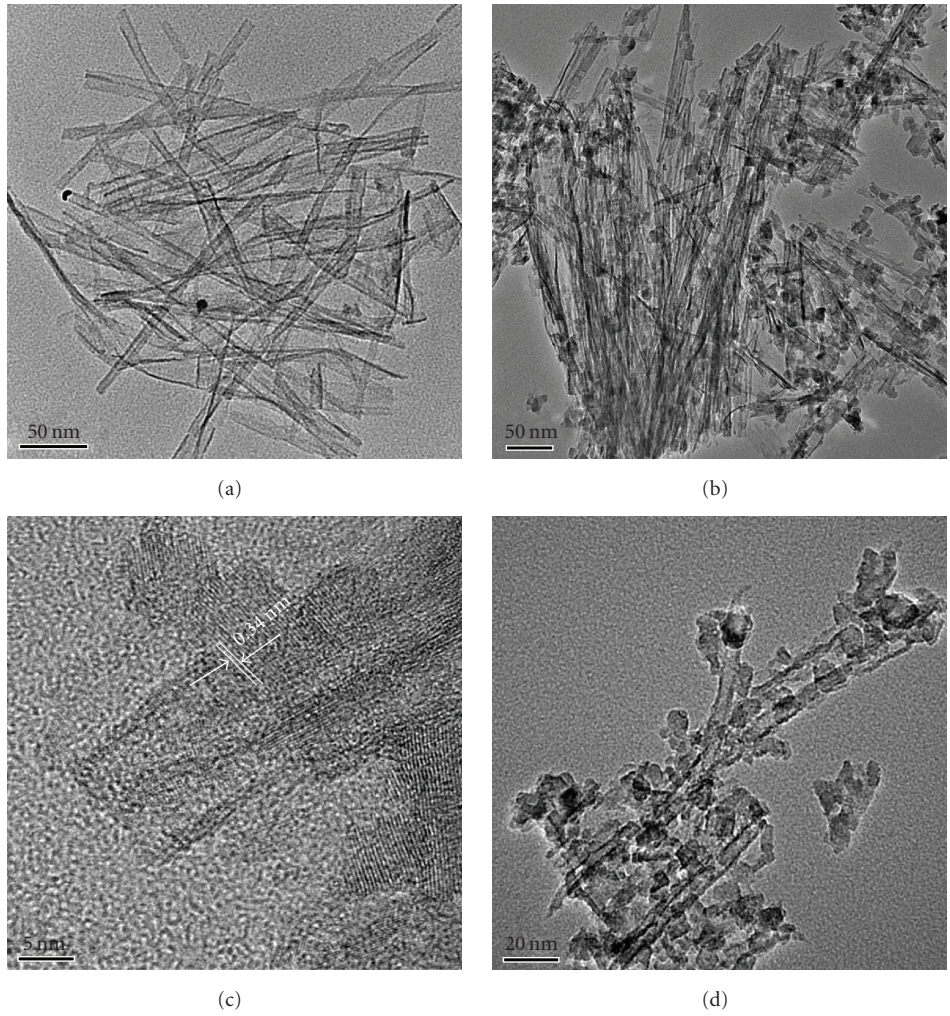

(a) (b)

(c) (d)

Figure 2: TEM images of TNTs (a) and TNTs-0-100 (b), HRTEM image of TNTs-0-100 (c), and TEM image of TNTs-23-120 (d).

17.8 nm to 12 nm. It might be related to the decreasing quantity of the TNTs and the increase of the TiO_2 crystallite size with the elevated temperature.

3.3. Photocatalytic Activity. The photocatalytic activities of the as-prepared catalysts were investigated by the photooxidation of two organic pollutants: ARG and phenol. The percentage of residual organic pollutants in water at different illumination times was studied. The photocatalytic activities of the pristine TNTs and the TNTs steamed at different temperature were compared, and the results were illustrated in Figure 4, where C referred to the residual concentration of aqueous organic pollutants at different reaction time and C_0 referred to the initial concentration of aqueous organic pollutants. The photodegradation of ARG in the 20 minutes prior to UV illumination was related to the dark adsorption process of aqueous ARG by the catalysts. According to the trend, the pristine TiO_2 nanotubes showed a very poor activity. As the vapor hydrolysis temperature was elevated, an enhancement in the degradation rate was achieved. It might be attributed to the improved crystallinity of the TNTs.

The photocatalytic activities of TiO_2 nanoparticles/ nanotubes composites with different content of TiO_2 loading at 120°C were also studied, and the degradation of ARG with the bare TiO_2 nanoparticles prepared at 120°C and the commercial TiO_2 (Degussa P25) was tested for the comparison. As presented in Figure 5, it could be found that all the nanotubes modified by TiO_2 nanoparticles exhibited the enhanced photocatalytic performances compared to TNTs-0-120 and the bare TiO_2 nanoparticles. As the TiO_2 loading amounts increased, the photocatalytic activities of the composites had improved and TNTs-50-120 took the shortest photooxidation time, which was close to that of Degussa P25. The bare TiO_2 nanoparticles were easy to agglomerate microspheres in size of $1\sim2\,\mu$m [27], and compared to the dispersed nanoparticles, the diffusion of ARD molecules into the interior of the spheres was more difficult. Also, the interior of microspheres was a much darker zone resulting from the scattering and absorption of the TiO_2 nanoparticles on the surface. So, the slow diffusion of ARG molecules and the poorer light harvesting resulted in the reduction of the photocatalytic efficiency of the bare

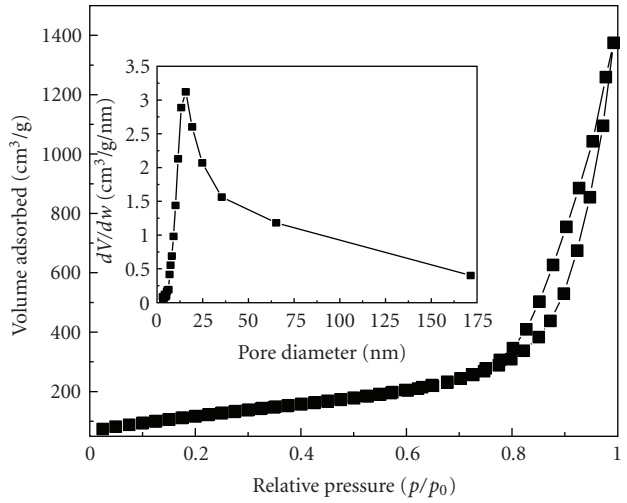

(a)

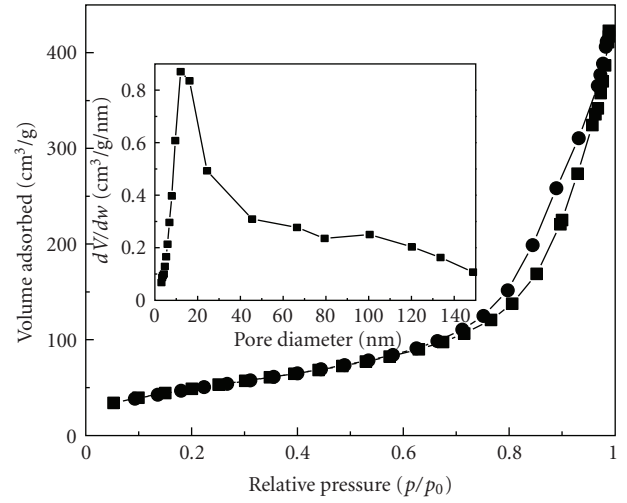

(b)

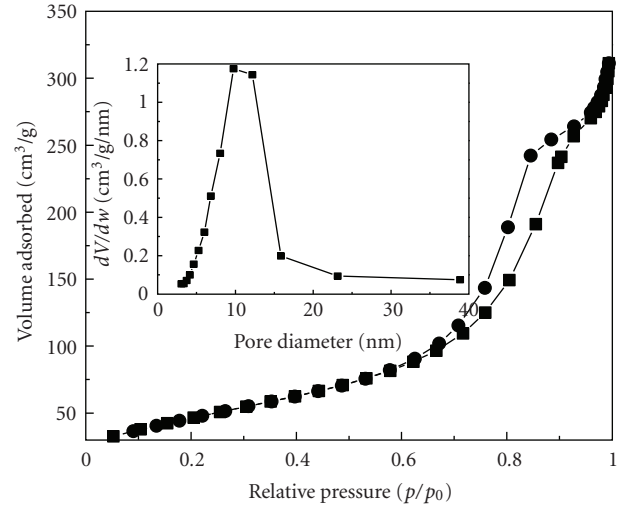

(c)

Figure 3: Nitrogen adsorption-desorption isotherm of the as-prepared samples with the corresponding pore size distribution curve inserted: TNTs (a), TNTs-0-120 (b), and TNTs-23-120 (c).

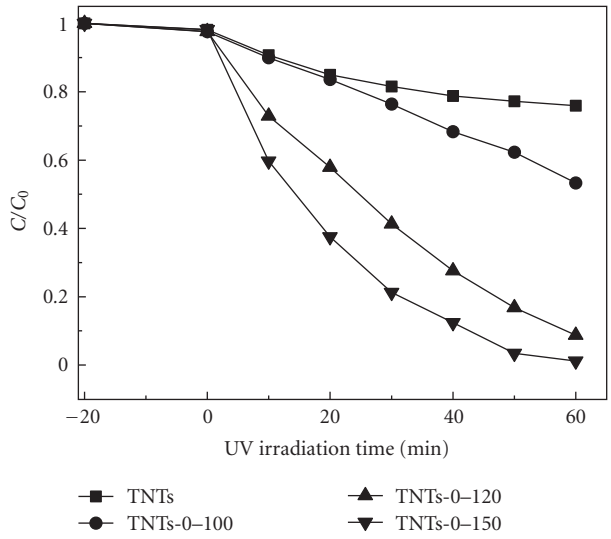

Figure 4: The concentration changes in ARG (50 ppm) over the catalysts under different experimental temperature.

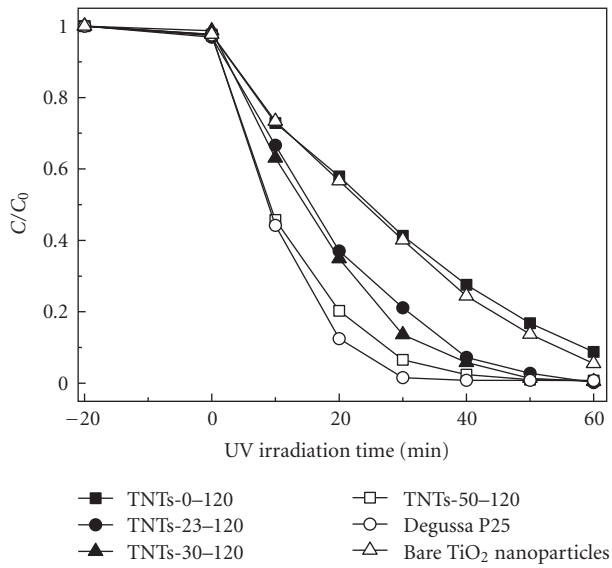

Figure 5: The concentration changes in ARG (50 ppm) over the composites with different content of TiO_2 loadings, Degussa P25 and the bare TiO_2 nanoparticles prepared at 120°C.

TiO_2 microspheres. However, in the preparation of TiO_2 nanoparticles/nanotubes composites, the TiO_2 nanoparticles could be highly dispersed on the surface of the nanotubes and the utilization of TiO_2 in photocatalysis had been raised. The mesoporous structure of the composites also provided more channels to adsorb dye molecules. In addition, in this work, the walls of TiO_2 nanotubes were composed of anatase TiO_2 nanoparticles which helped to capture the conduction band electrons. When irradiated with UV light, the well-crystallized TiO_2 nanocrystals would reduce the recombination of photogenerated electron-hole pairs

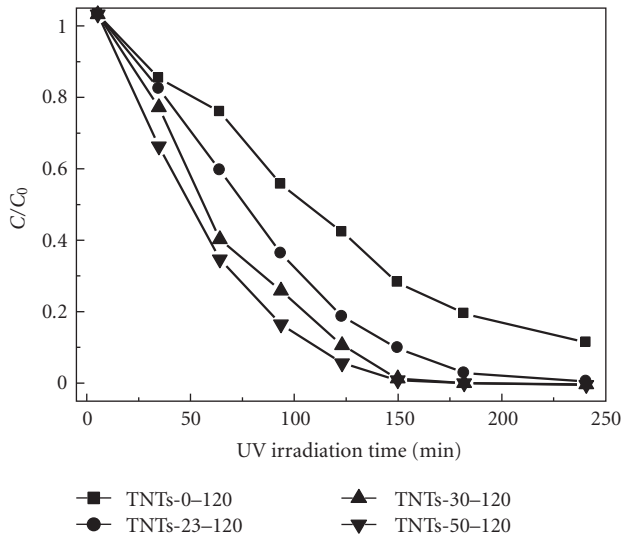

Figure 6: The concentration changes in phenol (50 ppm) over the composites with different content of TiO_2 loadings.

and the open-ended nanotubes would allow photons and reactants easy access to the nanotube surface [13]. Both the effects led to the enhanced photocatalytic efficiency.

Contrary to dyes, phenol is more difficult to degrade. Figure 6 shows the photocatalytic degradation rate of 50 ppm phenol solution using the modified composites with different TiO_2 loading amounts at 120°C. It took nearly 100 minutes for TNTs-0-120 to degrade 50% of the phenol solution. After loading with TiO_2 nanoparticles, the photocatalytic activities of the composites improved greatly. It took only 50 minutes for TNTs-50-120 to degrade 50% of the phenol solution, and it was attributed to the increase of active surface sites. The amount of TiO_2 loadings and the crystallization level of the composites were crucial to the improvement of photocatalytic efficiency. All the results demonstrated that the as-prepared TiO_2 nanoparticle/nanotube composites with enhanced photocatalytic activity were appropriate for the application in the degradation of organic pollutants.

4. Conclusion

In summary, TiO_2 nanoparticle/nanotube composites were synthesized via a vapor hydrolysis method in the presence of TNTs as a support. Since the open-ended TNTs had a large surface area and interstitial region, the anatase TiO_2 nanoparticles which provided more photoelectrons and holes to join the photocatalytic reaction could adhere to the surface of them at random. In addition, the walls of the TNTs were also composed of anatase TiO_2 nanoparticles. They could help to capture the conduction band electrons. Both the effects led the composites to show the improved photocatalytic activities for the degradation of organic pollutants under UV illumination, and the sample with 50 wt% of TiO_2 loading heated at 120°C obtained the highest photocatalytic activity.

Acknowledgment

This research was supported by the National Key Technology R and D Program (no. 2006BAA04B02-01), Research Fund for the Doctoral Program of Higher Education of China (no. 20100075110005), Shanghai Leading Academic Discipline Project (B603), and the Cultivation Fund of the Key Scientific and Technical Innovation Project (no. 708039).

References

[1] D. J. Yang, Z. F. Zheng, H. Y. Zhu, H. W. Liu, and X. P. Gao, "Titanate nanofibers as intelligent absorbents for the removal of radioactive ions from water," *Advanced Materials*, vol. 20, no. 14, pp. 2777–2781, 2008.

[2] S. Fukahori, H. Ichiura, T. Kitaoka, and H. Tanaka, "Photocatalytic decomposition of bisphenol A in water using composite TiO_2-zeolite sheets prepared by a papermaking technique," *Environmental Science and Technology*, vol. 37, no. 5, pp. 1048–1051, 2003.

[3] R. S. Yuan, J. T. Zheng, R. B. Guan, and Y. C. Zhao, "Surface characteristics and photocatalytic activity of TiO_2 loaded on activated carbon fibers," *Colloids and Surfaces A*, vol. 254, no. 1–3, pp. 131–136, 2005.

[4] P. Pucher, M. Benmami, R. Azouani et al., "Nano-TiO_2 sols immobilized on porous silica as new efficient photocatalyst," *Applied Catalysis A*, vol. 332, no. 2, pp. 297–303, 2007.

[5] G. M. Guo, B. B. Yu, P. Yu, and X. Chen, "Synthesis and photocatalytic applications of Ag/TiO_2-nanotubes," *Talanta*, vol. 79, no. 3, pp. 570–575, 2009.

[6] A. G. S. Prado and L. L. Costa, "Photocatalytic decouloration of malachite green dye by application of $TiO2_2$ nanotubes," *Journal of Hazardous Materials*, vol. 169, no. 1–3, pp. 297–301, 2009.

[7] C. Ratanatawanate, Y. Tao, and K. J. Balkus, "Photocatalytic activity of PbS quantum dot/TiO_2 nanotube composites," *Journal of Physical Chemistry C*, vol. 113, no. 24, pp. 10755–10760, 2009.

[8] H. Q. An, J. Zhou, J. X. Li et al., "Deposition of Pt on the stable nanotubular TiO_2 and its photocatalytic performance," *Catalysis Communications*, vol. 11, no. 3, pp. 175–179, 2009.

[9] L. H. Huang, C. Sun, and Y. L. Liu, "Pt/N-codoped TiO_2 nanotubes and its photocatalytic activity under visible light," *Applied Surface Science*, vol. 253, no. 17, pp. 7029–7035, 2007.

[10] L. S. Wang, M. W. Xiao, X. J. Huang, and Y. D. Wu, "Synthesis, characterization, and photocatalytic activities of titanate nanotubes surface-decorated by zinc oxide nanoparticles," *Journal of Hazardous Materials*, vol. 161, no. 1, pp. 49–54, 2009.

[11] T. Akita, M. Okumura, K. Tanaka et al., "Transmission electron microscopy observation of the structure of TiO_2 nanotube and Au/TiO_2 nanotube catalyst," *Surface and Interface Analysis*, vol. 37, no. 2, pp. 265–269, 2005.

[12] S. Shamaila, A. K. L. Sajjad, F. Chen, and J. L. Zhang, "Study on highly visible light active Bi_2O_3 loaded ordered mesoporous titania," *Applied Catalysis B*, vol. 94, no. 3-4, pp. 272–280, 2010.

[13] T. Wang, S. Wang, W. X. Chen et al., "Chemical morphology freezing: chemical protection of the physical morphology of high photoactivity anatase TiO_2 nanotubes," *Journal of Materials Chemistry*, vol. 19, no. 27, pp. 4692–4694, 2009.

[14] J. C. Xu, M. Lu, X. Y. Guo, and H. L. Li, "Zinc ions surface-doped titanium dioxide nanotubes and its photocatalysis activity for degradation of methyl orange in water," *Journal of Molecular Catalysis A*, vol. 226, no. 1, pp. 123–127, 2005.

[15] Q. Zhao, M. Li, J. Y. Chu, T. Jiang, and H. B. Yin, "Preparation, characterization of Au (or Pt)-loaded titania nanotubes and their photocatalytic activities for degradation of methyl orange," *Applied Surface Science*, vol. 255, no. 6, pp. 3773–3778, 2009.

[16] S. H. Chien, Y. C. Liou, and M. C. Kuo, "Preparation and characterization of nanosized Pt/Au particles on TiO_2-nanotubes," *Synthetic Metals*, vol. 152, no. 1–3, pp. 333–336, 2005.

[17] V. Loddo, G. Marcì, C. Martín, L. Palmisano, V. Rives, and A. Sclafani, "Preparation and characterisation of TiO_2 (anatase) supported on TiO_2 (rutile) catalysts employed for 4-nitrophenol photodegradation in aqueous medium and comparison with TiO_2 (anatase) supported on Al_2O_3," *Applied Catalysis B*, vol. 20, no. 1, pp. 29–45, 1999.

[18] C. S. Guo, M. Ge, L. Liu, G. Gao, Y. C. Feng, and Y. Q. Wang, "Directed synthesis of mesoporous TiO_2 microspheres: catalysts and their photocatalysis for bisphenol A degradation," *Environmental Science and Technology*, vol. 44, no. 1, pp. 419–425, 2010.

[19] Q. H. Zhang, L. Gao, J. Sun, and S. Zheng, "Preparation of long TiO_2 nanotubes from ultrafine rutile nanocrystals," *Chemistry Letters*, vol. 31, no. 2, pp. 226–227, 2002.

[20] D. V. Bavykin, V. N. Parmon, A. A. Lapkin, and F. C. Walsh, "The effect of hydrothermal conditions on the mesoporous structure of TiO_2 nanotubes," *Journal of Materials Chemistry*, vol. 14, no. 22, pp. 3370–3377, 2004.

[21] Q. Y. Li, T. Kako, and J. H. Ye, "Strong adsorption and effective photocatalytic activities of one-dimensional nano-structured silver titanates," *Applied Catalysis A*, vol. 375, no. 1, pp. 85–91, 2010.

[22] S. Nosheen, F. S. Galasso, and S. L. Suib, "Role of Ti-O bonds in phase transitions of TiO_2," *Langmuir*, vol. 25, no. 13, pp. 7623–7630, 2009.

[23] J. H. Jiang, Q. M. Gao, and Z. Chen, "Gold nanocatalysts supported on protonic titanate nanotubes and titania nanocrystals," *Journal of Molecular Catalysis A*, vol. 280, no. 1-2, pp. 233–239, 2008.

[24] Y. M. Xu, X. M. Fang, and Z. G. Zhang, "Formation of single-crystalline TiO_2 nanomaterials with controlled phase composition and morphology and the application in dye-sensitized solar cell," *Applied Surface Science*, vol. 255, no. 21, pp. 8743–8749, 2009.

[25] L. Torrente-Murciano, A. A. Lapkin, D. V. Bavykin, and F. C. Walsh, "Highly selective Pd/titanate nanotube catalysts for the double-bond migration reaction," *Journal of Catalysis*, vol. 245, no. 2, pp. 272–278, 2007.

[26] M. A. Khan, M. S. Akhtar, S. I. Woo, and O. B. Yang, "Enhanced photoresponse under visible light in Pt ionized TiO_2 nanotube for the photocatalytic splitting of water," *Catalysis Communications*, vol. 10, no. 1, pp. 1–5, 2008.

[27] Z. L. Wang, L. Q. Mao, and J. Lin, "Preparation of TiO_2 nanocrystallites by hydrolyzing with gaseous water and their photocatalytic activity," *Journal of Photochemistry and Photobiology A*, vol. 177, no. 2-3, pp. 261–268, 2006.

[28] J. G. Yu, G. Wang, B. H. Cheng, and M. H. Zhou, "Effects of hydrothermal temperature and time on the photocatalytic activity and microstructures of bimodal mesoporous TiO_2 powders," *Applied Catalysis B*, vol. 69, no. 3-4, pp. 171–180, 2007.